JACS
JOURNAL OF THE AMERICAN CHEMICAL SOCIETY

COMMUNICATION

pubs.acs.org/JACS

The Dynamics of Unfolded versus Folded tRNA: The Role of Electrostatic Interactions

Joon Ho Roh,[*,†,‡,§] Madhu Tyagi,[†,§] R. M. Briber,[*,†] Sarah A. Woodson,[*,‡] and Alexei P. Sokolov[||,⊥]

[†]Department of Materials Science and Engineering, University of Maryland, College Park, Maryland, United States
[‡]T. C. Jenkins Department of Biophysics, Johns Hopkins University, Baltimore, Maryland, United States
[§]NIST Center for Neutron Research, National Institute of Standards and Technology, Gaithersburg, Maryland, United States
[||]Chemical Science Division, Oak Ridge National Laboratory, Oak Ridge, Tennessee, United States
[⊥]Department of Chemistry, University of Tennessee, Knoxville, Tennessee, United States

Supporting Information

ABSTRACT: The dynamics of RNA contributes to its biological functions such as ligand recognition and catalysis. Using quasielastic neutron scattering spectroscopy, we show that Mg^{2+} greatly increases the picosecond to nanosecond dynamics of hydrated tRNA while stabilizing its folded structure. Analyses of the atomic mean-squared displacement, relaxation time, persistence length, and fraction of mobile atoms showed that unfolded tRNA is more rigid than folded tRNA. This same result was found for a sulfonated polystyrene, indicating that the increased dynamics in Mg^{2+} arises from improved charge screening of the polyelectrolyte rather than specific interactions with the folded tRNA. These results are opposite to the relationship between structural compactness and internal dynamics for proteins in which the folded state is more rigid than the denatured state. We conclude that RNA dynamics are strongly influenced by the electrostatic environment, in addition to the motions of local waters.

Understanding the dynamic interactions between biological macromolecules in their local hydration environment is critical for mapping out the physical basis of biological events such as enzymatic function[1] and folding pathways.[2] Numerous neutron scattering and simulation studies have reported that motions in proteins are controlled by the dynamics of hydrating water rather than by the intrinsic dynamics of the polypeptide chain.[3] More recently, it has become clear that the dynamics of charged biological macromolecules are more complex than previously thought, involving nontrivial electrostatic fluctuations of charged groups which are strongly influenced by the local ionic environment.[4]

The dynamics of RNA presents a special challenge, as cations that cluster around the negatively charged polynucleotide stabilize the folded structure of the RNA while neutralizing the negative charge and interacting with hydrating water molecules.[5] Efforts to understand how the internal dynamics varies in response to different electrostatic environments, and the structural ramifications of the dynamics, are just beginning.[6] This Communication reports that the local dynamics of tRNA strongly increases in the presence of Mg^{2+} ions, which stabilize the folded structure while altering the electrostatic environment around the tRNA. Interestingly, this observation is opposite to what has been reported for proteins where the folded state is observed to be more rigid than the unfolded state.[2b−d] We also observe a similarity in the effect of charge screening on the dynamical properties between tRNA and a synthetic polyelectrolyte. This implies that electrostatic interactions are a key factor in determining the local dynamics of polyelectrolytes.

Our recent neutron scattering and dielectric studies showed that the conformational dynamics of hydrated DNA, RNA, and protein samples vary differently with temperature, suggesting that the observed motions arise from a mutual response between water and the biological macromolecules.[4b,7] In this view, chemical structure, water density, and electrostatic environment contribute collectively to the local dynamics. Therefore, in order to directly probe electrostatic effects on the local dynamics, we performed experiments designed to minimize physical differences other than the electrostatic potential.[4b] In this work we report on the investigation of the dynamics of unfolded tRNA (u-tRNA) under low ionic strength and folded tRNA (f-tRNA) in $MgCl_2$ measured using quasielastic neutron scattering spectroscopy. We also carried out similar experiments on a charged synthetic polyelectrolyte that does not fold into a specific structure in the presence of Mg^{2+} cations.

Wheat germ tRNA was prepared as described in the Supporting Information (SI). Most tRNAs form some stable secondary structure (Watson−Crick base pairs) at low ionic strength, despite the electrostatic repulsion of the phosphates.[8] Electrostatic neutralization by small amounts of multivalent cations such as Mg^{2+} enables tRNA to fold into a compact structure that contains tertiary interactions.[8,9] Thus, u-tRNA prepared from a low ionic strength solution was expected to only form secondary structures, while f-tRNA prepared with $MgCl_2$ (~0.4 mol per mole of phosphate) was expected to also form tertiary structures.[8−10]

For powder samples, tRNAs were equilibrated with D_2O until the first hydration layer was filled (see SI for details about sample preparation). We estimate that the solvent-accessible surface area[11] of unfolded tRNA is only 4% greater than that of the folded tRNA (Figure S2 and Table S1). Thus, the u-tRNA and f-tRNA contain approximately the same amount of water in the first hydration shell.

Received: August 13, 2011
Published: September 21, 2011

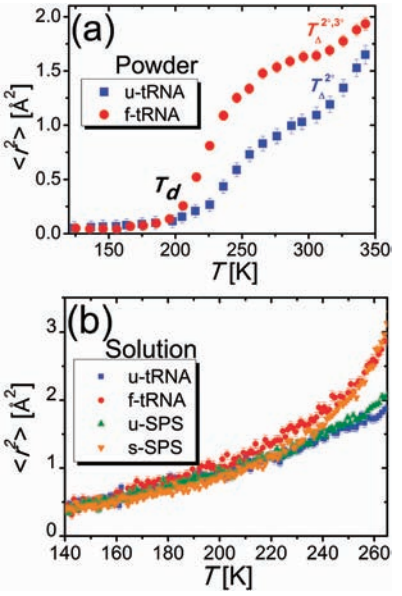

Figure 1. Temperature dependence of the mean-squared displacement, $\langle r^2(T)\rangle$, obtained from a Gaussian approximation, $\langle r^2(T)\rangle = -3Q^{-2}\ln[I_{el}(Q,T)/I_{el}(Q,50\,\mathrm{K})]$ for Q between 0.25 and 1.00 Å^{-1}. (a) Powder u- and f-tRNA samples were hydrated to 42% (w/w). The dynamic transition ($T_d \approx 200$ K) and melting transition ($T_\Delta^{2°3°} \approx 325$ K) are indicated. No water crystallization appeared in the hydrated powder samples (see Figures S4 and S5). The plateau of $\langle r^2\rangle$ values at $T \approx 300$ K is probably because of the appearance of relaxation modes responsible for the dynamic transition (T_d) into the given time window.[15] The melting transition is associated with the disruption of heterogeneous secondary structures and the tertiary structure of tRNAs.[16] (b) D_2O solutions of u- and f-tRNA and u- and s-SPS. Resolving the sample dynamics at $T > 260$ K is not possible due to strong scattering from water crystallization at ~270 K and the motions of D_2O at this higher temperature range. Error bars throughout the text represent one standard deviation.

Neutron scattering measurements were performed using the high-flux back-scattering spectrometer at the NIST Center for Neutron Research (energy resolution ~1 μeV ~ 2 ns).[12] Elastic scattering scans were carried out during cooling from 300 to 50 K, and upon heating from 300 to 350 K (heating/cooling rate: 0.7 K/min). Energy-resolved spectra were measured in the energy range ±17 μeV (~40 ps). Since the incoherent neutron scattering cross section of hydrogen is 40 times larger than that of deuterium, we primarily observe the motions of nonexchangeable hydrogen atoms in the tRNA.[13] Neutron scattering data were reduced and analyzed using DAVE software.[14]

Figure 1A shows that the dynamic transition (T_d) associated with the onset of anharmonic motions within the resolution window of the spectrometer[15] appears in both u- and f-tRNA samples at $T \approx 180-200$ K. Another transition at $T \approx 325$ K correlates with initial melting of tRNA secondary (2°) and tertiary (3°) structures.[16] Since the full melting transition is not visible in the neutron scattering measurements, the denaturing temperature, T_Δ, is empirically determined from first derivative of $\langle r^2\rangle$. UV absorption measurements as a function of temperature confirmed the appearance of a broad melting transition in u-tRNA and f-tRNA samples (Figure S6).

Strikingly, the $\langle r^2\rangle$ values of the compact f-tRNA were larger than those of the extended u-tRNA at all temperatures up to 350 K. In addition, $\langle r^2\rangle$ increased much more rapidly between 200 and 250 K for f-tRNA than for u-tRNA (Figure 1A). The different temperature dependence of the conformational mobility between u- and f-tRNA implies that the observed dynamics are not controlled solely by the dynamics of the hydrating water but are significantly affected by the electrostatic nature of the RNA surface.

To gain insight into whether Mg^{2+} affects tRNA flexibility by stabilizing the tertiary structure or by changing the electrostatic environment, we measured the dynamical flexibility of sulfonated polystyrene (SPS) with and without Mg^{2+} (see SI for details about sample preparation). Like tRNA, Mg^{2+}-screened SPS (s-SPS) experienced larger local motion (i.e., larger $\langle r^2\rangle$) compared to unscreened SPS (u-SPS) (Figure 1B). The larger $\langle r^2\rangle$ values of s-SPS and f-tRNA compared with those of low ionic strength samples indicate that the electrostatic neutralization by Mg^{2+} results in larger or more thermal fluctuations of the polyelectrolyte. It is striking that $\langle r^2\rangle$ values of a biological and a synthetic polyelectrolyte increase similarly with temperature in both the unscreened and Mg^{2+}-screened conditions.

Because the samples in this study have similar hydration levels, the differences we observe are primarily due to Mg^{2+}. Together with our earlier results, this suggests that the dynamical properties of biological polyelectrolytes are mainly controlled by solvation and electrostatics, rather than specific macromolecular structure.[2d,17]

To understand the physical basis of the RNA−water coupled motions, we acquired dynamic structure factors, $S(Q,E)$, of u- and f-tRNA at different temperatures. The total scattering spectra can be represented as

$$S(Q,E) = \mathrm{DW}(Q)[(1-\mathrm{QISF}(Q))\delta(E) + \mathrm{QISF}(Q)S_{\mathrm{QENS}}(Q,E)] \otimes R(E) \quad (1)$$

Here, DW(Q) is the Debye−Waller factor, QISF(Q) is the quasielastic incoherent scattering factor, defined as the ratio of quasielastic scattering to the total scattering intensity, $S_{\mathrm{QENS}}(Q,E)$ is a quasielastic scattering function, and $R(E)$ is a resolution function. The amplitude of QISF is directly proportional to the mobile fraction of hydrogen atoms associated with the relaxation. We used $S(Q,E)$ obtained at 10 K as a resolution function.

Figure 2 shows that $S(Q,E)$ exhibits about a factor of 2 larger quasielastic scattering from f-tRNA than u-tRNA from 260 to 320 K over a wide range of transferred energy. This indicates that f-tRNA experiences a larger mobile fraction with faster conformational motions (Figure 3 and Figure S7). Quasielastic scattering of u-tRNA at 350 K becomes similar to that of f-tRNA at 300 K, which agrees with the sharp increase in $\langle r^2\rangle$ for u-tRNA between 325 and 350 K as the secondary structure begins to melt. However, the u-tRNA remains less mobile than f-tRNA at temperatures above the melting transition (Figures 1A and 2B).

The characteristic relaxation time, $\langle\tau_R\rangle$, of the tRNA atomic motions was estimated from the half-width at half-maximum of $S_{\mathrm{QENS}}(Q,E)$, fit to a single Lorentzian. Although the single Lorentzian fit is not the best analysis of a stretched relaxation spectrum, it provides a qualitative comparison of $\langle\tau_R\rangle$ values within the limit of the given time window,[13] especially for RNA molecules that lack methyl groups.[7,18] We stress that the $\langle\tau_R\rangle$ values estimated in this way do not represent the real relaxation times, and a more accurate analysis of the relaxation times will require broader frequency range spectra from multiple spectrometers (e.g., refs 4b and 15).

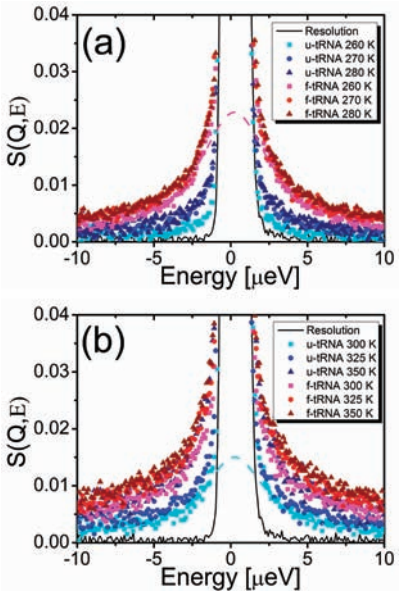

Figure 2. Dynamic structure factor, $S(Q = 0.56\,\text{Å}^{-1},E)$, of u- and f-tRNA at various temperatures. Resolution functions are $S(Q = 0.56\,\text{Å}^{-1},E)$ at 10 K. Dashed lines are representative Lorentzian fits of quasielastic scattering of f-tRNA at 260 K and u-tRNA at 300 K using eq 1.

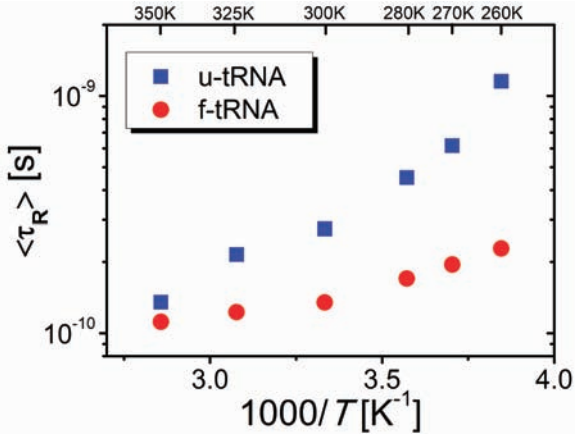

Figure 3. Averaged relaxation time, $\langle\tau_R\rangle$, of u- and f-tRNA obtained from deconvoluting $S(Q = 0.56\,\text{Å}^{-1},E)$ into Lorentzian quasielastic and Gaussian elastic peaks. The $\langle\tau_R\rangle$ value was estimated from half-width at half-maximum of a Lorentzian peak. Since the energy range is limited to 40 ps and 2 ns, the $\langle\tau_R\rangle$ values do not represent the absolute relaxation time. No significant Q-dependence of the $\langle\tau_R\rangle$ values was found, indicating that the relaxation is localized.

Analysis of the QENS data shows that $\langle\tau_R\rangle$ of u-tRNA is generally slower and more temperature-dependent than $\langle\tau_R\rangle$ of f-tRNA (Figure 3). The average relaxation rate of u-tRNA becomes about 1 order of magnitude slower than that of f-tRNA at $T \approx 260$ K. Likewise, the QISF of u-tRNA is also lower than that of f-tRNA, suggesting the chain is less dynamically active (Figures S7 and S8). Therefore, u- and f-tRNAs experience different dynamical pathways, although they have similar dynamical transitions, T_d. These results indicate that water likely serves as a plasticizer that lubricates conformational motions of the macromolecules.[7]

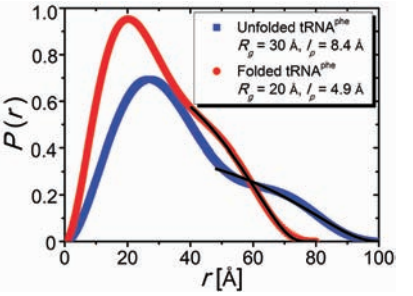

Figure 4. Analysis of pair distance distribution functions, $P(r)$, of unfolded and folded tRNA^{Phe}. $P(r)$ was obtained from indirect inverse Fourier transform of small-angle X-ray scattering intensity using the GNOM program.[10] The radius of gyration, R_g, and persistence length, l_p, were estimated from $P(r)$ (see SI).[10,19a] Black lines are the fits of $P(r)$ to the exponential equation (Eq. S2) at $r > R_g$ on the basis of a worm-like chain model.[19a]

At this point, it is worth addressing why folded RNA ($R_g \approx$ 20 Å for tRNA^{Phe})[10] with long-range tertiary interactions has larger dynamical flexibility than unfolded RNA ($R_g \approx 30$ Å for tRNA^{Phe}).[10] This observation is contrary to the relationship between structural compactness and global dynamics that holds for folded proteins, which are more rigid than denatured proteins.[2b−d] Unlike proteins and neutral polymers, hydrated RNA and DNA are stiff at low ionic strength because of the electrostatic repulsion of the negatively charged phosphates.[19] Our estimate of the persistence length, l_p, from solution scattering (Figure 4) showed that l_p is 1.7 times larger for u-tRNA compared to f-tRNA (8.4 vs 4.9 Å), indicating significantly higher flexibility for the folded tRNA. This result also agrees with the dependence of persistence length of RNA on salt.[19a] The difference in persistence length is consistent with the difference in $\langle r^2\rangle$ between f- and u-tRNA at T = 300 K (Figure 1A).[7] Furthermore, previous work showed that SPS also becomes more compact and more flexible in Mg^{2+}, although it does not form a specific structure.[17]

Our study demonstrates that charge screening due to the presence of counterions greatly increases the local motion of tRNA and a synthetic polyelectrolyte. The concerted increase in the magnitude of the displacement, relaxation rate, and fraction of mobile atoms observed by neutron spectroscopy correlates with greater flexibility of the tRNA backbone and is additionally reflected in the shorter persistence length of the folded tRNA. The mechanism by which Mg^{2+} increases the flexibility of the compact f-tRNA is not well understood. Molecular simulations suggest that motions in the nanosecond to picosecond range in tRNA are associated with high-frequency hinge-bending modes and fluctuations in the anticodon loop and 3′ acceptor.[7,20] Possible scenarios explaining the increased dynamics of f-tRNA relative to u-tRNA include (1) increased electrostatic fluctuations caused by the diffusion of hydrated cations in the vicinity of the tRNA and (2) increased fluctuations of the hydrogen bond network between the screened backbone and hydrating water. Further studies are needed on the relative importance of counterion diffusion, ion−ion correlations, and hydrogen bond fluctuations. Interestingly, NMR,[6a] birefringence,[21] and molecular dynamics simulation[20c] studies concluded that Mg^{2+} reduces the mobility of single-stranded RNA segments compared to monovalent cations. More details about the electrostatic origins of tRNA dynamics should be obtained through the comparison of dynamics in the

presence of monovalent cations with different ionic densities, such as Na^+ and K^+.[4a]

■ ASSOCIATED CONTENT

Supporting Information. Detailed sample preparation; estimate of solvent-accessible surface area; elastic incoherent scattering factor; intermediate scattering function; and titration of UV absorption measurements. This material is available free of charge via the Internet at http://pubs.acs.org.

■ AUTHOR INFORMATION

Corresponding Author
rohmio1973@gmail.com; rbriber@umd.edu; swoodson@jhu.edu

■ ACKNOWLEDGMENT

We thank T. Sosnick for providing small-angle X-ray scattering data of $tRNA^{Phe}$ from which the values of persistence length were estimated. J.H.R., R.M.B., and S.A.W. acknowledge support from DOC-NIST through the cooperative agreement 70NANB7H6177. A.P.S. acknowledges DOE support through EPSCoR program (grant DE-FG02-08ER46528). This work used facilities at the NCNR supported in part by the National Science Foundation under Agreement No. DMR-0944772.

■ REFERENCES

(1) (a) Rasmussen, B. F.; Stock, A. M.; Ringe, D.; Petsko, G. A. *Nature* **1992**, *357*, 423. (b) Rupley, J. A.; Careri, G. *Adv. Protein Chem.* **1991**, *41*, 37. (c) Doster, W.; Cusack, S.; Petry, W. *Nature* **1989**, *337*, 754. (d) Westhof, E. *Annu. Rev. Biophys. Biophys. Chem.* **1988**, *17*, 125.

(2) (a) Bu, Z.; Cook, J.; Callaway, D. J. E. *J. Mol. Biol.* **2001**, *312*, 865. (b) Receveur, V.; Calmettes, P.; Smith, J. C.; Desmadril, M.; Coddens, G.; Durand, D. *Proteins: Struct., Funct., Genet.* **1997**, *28*, 380. (c) Bu, Z.; Neumann, D. A.; Lee, S.-H.; Brown, C. M.; Engelman, D. M.; Han, C. C. *J. Mol. Biol.* **2000**, *301*, 525. (d) Mamontov, E.; O'Neill, H.; Zhang, Q. *J. Biol. Phys.* **2010**, *36*, 291.

(3) (a) Beece, D.; Eisenstein, L.; Frauenfelder, H.; Good, D.; Marden, M. C.; Reinisch, L.; Reynolds, A. H.; Sorensen, L. B.; Yue, K. T. *Biochemistry* **1980**, *19*, 5147. (b) Fenimore, P. W.; Frauenfelder, H.; McMahon, B. H.; Parak, F. G. *Proc. Natl. Acad. Sci. U.S.A.* **2002**, *99*, 16047. (c) Tournier, A. L.; Xu, J. C.; Smith, J. C. *Biophys. J.* **2003**, *85*, 1871. (d) Vitkup, D.; Ringe, D.; Petsko, G. A.; Karplus, M. *Nat. Struct. Biol.* **2000**, *7*, 34. (e) Wood, K.; Frolich, A.; Paciaroni, A.; Moulin, M.; Hartlein, M.; Zaccai, G.; Tobias, D. J.; Weik, M. *J. Am. Chem. Soc.* **2008**, *130*, 4586.

(4) (a) Zaccai, G. *Philos. Trans. R. Soc. London Ser. B-Biol. Sci.* **2004**, *359*, 1269. (b) Khodadadi, S.; Roh, J. H.; Kisliuk, A.; Mamontov, E.; Tyagi, M.; Woodson, S. A.; Briber, R. M.; Sokolov, A. P. *Biophys. J.* **2010**, *98*, 1321. (c) Wood, K.; Plazanet, M.; Gabel, F.; Kessler, B.; Oesterhel, D.; Tobias, D. J.; Zaccai, G.; Weik, M. *Proc. Natl. Acad. Sci. U.S.A.* **2007**, *104*, 18049. (d) Li, X.; Zamponi, M.; Hong, K.; Porcar, L.; Shew, C.-Y.; Jenkins, T.; Liu, E.; Smith, G. S.; Herwig, K. W.; Liu, Y.; Chen, W.-R. *Soft Matter* **2011**, *7*, 618.

(5) (a) Woodson, S. A. *Curr. Opin. Chem. Biol.* **2005**, *9*, 104. (b) Draper, D. E.; Grilley, D.; Soto, A. M. *Annu. Rev. Biophys. Biomol. Struct.* **2005**, *34*, 221.

(6) (a) Getz, M.; Sun, X.; Casiano-Negroni, A.; Zhang, Q.; Al-Hashimi, H. M. *Biopolymers* **2007**, *86*, 384. (b) Bailor, M.; Sun, X.; Al-Hashimi, H. M. *Science* **2010**, *327*, 202.

(7) Roh, J. H.; Briber, R. M.; Damjanovic, A.; Thirumalai, D.; Woodson, S. A.; Sokolov, A. P. *Biophys. J.* **2009**, *96*, 2755.

(8) Schimmel, P. R.; Redfield, A. G. *Annu. Rev. Biophys. Bioeng.* **1980**, *9*, 181.

(9) Stein, A.; Crothers, D. M. *Biochemistry* **1976**, *15*, 160.

(10) Fang, X. W.; Littrell, K.; Yang, X.; Henderson, S. J.; Siefert, S.; Thiyagarajan, P.; Pan, T.; Sosnick, T. R. *Biochemistry* **2000**, *39*, 11107.

(11) Cavallo, L.; Kleinjung, J.; Fraternali, F. *Nucleic Acids Res.* **2003**, *31*, 3364.

(12) Meyer, A.; Dimeo, R. M.; Gehring, P. M.; Neumann, D. A. *Rev. Sci. Instrum.* **2003**, *74*, 2759.

(13) Gabel, F.; Bicout, D.; Lehnert, U.; Tehei, M.; Weik, M.; Zaccai, G. *Q. Rev. Biophys.* **2002**, *35*, 327.

(14) Azuah, R. T.; Kneller, L. R.; Qiu, Y.; Tregenna-Piggott, P. L. W.; Copley, J. R. D.; Dimeo, R. M. *J. Res. Natl. Inst. Stand. Technol.* **2009**, *114*, 341.

(15) Khodadadi, S.; Pawlus, S.; Roh, J. H.; Sakai, V. G.; Mamontov, E.; Sokolov, A. P. *J. Chem. Phys.* **2008**, *128*, 5.

(16) (a) Tinonco, I., Jr.; Bustamante, C. *J. Mol. Biol.* **1999**, *293*, 271. (b) Bina-Stein, M.; Crothers, D. M.; Hilbers, C. W.; Shulman, R. G. *Proc. Natl. Acad. Sci. U.S.A.* **1976**, *73*, 2216.

(17) Zhang, Y.; Douglas, J. F.; Ermi, B. D.; Amis, E. J. *J. Chem. Phys.* **2001**, *114*, 3299.

(18) Roh, J. H.; Novikov, V. N.; Gregory, R. B.; Curtis, J. E.; Chowdhuri, Z.; Sokolov, A. P. *Phys. Rev. Lett.* **2005**, *95*, 038101-1.

(19) (a) Caliskan, G.; Hyeon, C.; Perez-Salas, U.; Briber, R. M.; Woodson, S. A.; Thirumalai, D. *Phys. Rev. Lett.* **2005**, *95*, 268303-1. (b) Hagerman, P. J. *Annu. Rev. Biophys. Struct.* **1997**, *26*, 139. (c) Gast, F.-U.; Hagerman, P. J. *Biochemistry* **1991**, *30*, 4268. (d) Kebbekus, P.; Draper, D. E. *Biochemistry* **1995**, *34*, 4354. (e) Abels, J. A.; Moreno-Herrero, F.; van der Heijden, T.; Dekker, C.; Dekker, N. H. *Biophys. J.* **2005**, *88*, 2737.

(20) (a) Nakamura, S.; Doi, J. *Nucleic Acids Res.* **1994**, *22*, 514. (b) Harvey, S. C.; Prabhakaran, M.; MacCammon, J. A. *Biopolymers* **1985**, *24*, 1169. (c) Auffinger, P.; Louise-May, S.; Westhof, E. *Biophys. J.* **1999**, *76*, 50.

(21) Friederich, M. W.; Vacano, E.; Hagerman, P. J. *Proc. Natl. Acad. Sci. U.S.A.* **1998**, *95*, 3572.